WORLD CONFERENCE ON TIMBER ENGINEERING 2025
BRISBANE, AUSTRALIA
Advancing Timber for the Future Built Environment

STUDY OF THE SLIP PERFORMANCE OF SCREWS IN *EUCALYPTUS NITENS* (*E. NITENS*) FROM TASMANIAN FIBRE-MANAGED PLANTATIONS

Zhiqian Zhong[1], Assaad Taoum[2], Nathan Kotlarewski[3], Gregory Nolan[4]

ABSTRACT: This study examines the influence of screw parameters, including effective screw thread bearing area per flank, thread angle, effective penetration length and screw-grain angle, as well as timber density on the axial slip performance of screws embedded in *Eucalyptus nitens* (*E. nitens*) timber. Six types of screw (G8, G10, SP5, SP6, G14, and SP8), totalling 544 screws, were tested in pull-out tests, with variations in thread bearing area (11 to 32 mm²), effective penetration length (25 to 75 mm), and screw-grain angle (0° to 90). The findings highlight that increasing effective penetration length significantly enhances axial slip modulus, with screws penetrating three-layer glued laminated timber (GLT) (75 mm) exhibiting the highest axial slip performance. Despite the lower timber density in the E3 timber series, penetration length proved to be a more dominant factor in axial slip modulus than density. Additionally, screws with larger thread bearing areas and smaller thread angles consistently demonstrated higher axial slip modulus, confirming its critical role in axial slip performance. Thread angle negatively impacted axial slip performance, with SPAX screws (35° thread angle) outperforming G-series screws (60° thread angle) due to their increased thread loading surface and reduced localised timber damage. The study further reveals that the relationship between screw-grain angle and axial slip modulus follows a parabolic trend, significantly influenced by effective penetration length, thread angle, and density simultaneously. These results underscore the importance of selecting screws with longer penetration lengths, larger thread bearing areas, and smaller thread angles to maximise connection stiffness.

KEYWORDS: fibre-managed timber, engineered wood products (EWP), *Eucalyptus nitens* (*E. nitens*), axial slip performance, screws

1 – INTRODUCTION

The growing emphasis on sustainability and efficiency in the construction industry has driven significant advancements in materials and structural systems. Among these, timber-based composite structures, such as Timber-Concrete Composite (TCC) and Timber-Steel Composite (TSC) systems, have garnered attention for their ability to enhance structural performance while reducing environmental impacts. TCC systems, in particular, leverage the complementary mechanical properties of timber and concrete to create resilient and durable structures, making them a popular choice in modern construction [1, 2]

A key factor in the success of these composite systems is the connectors, such as screws, which are crucial for ensuring a secure mechanical connection between different materials like timber and concrete. These fasteners play an integral role in transferring loads, maintaining composite action, and enhancing overall structural integrity [3]. Specifically, the performance of the connection system directly influences the structural behaviour and durability of composite systems under various loading conditions [4]. The efficiency and resilience of these connections are essential to maximising the potential of composite systems, as they dictate the degree of interaction between materials, ultimately affecting strength, stiffness, and deformation capacity [5]. Notably, inclined screws in the timber composite structure have demonstrated high slip resisting, further improving the mechanical performance of these systems [6].

According to EN1995-1-1 [7] and the formula proposed by Tomasi et al. [8],the slip modulus for screw-grain angle ranging from 0° to 90° is the combination of the axial slip modulus ($K_{SLS,ax}$) and the lateral slip modulus ($K_{SLS,v}$).

[1] Zhiqian Zhong, School of Engineering, University of Tasmania, Hobart, TAS 7005, Australia, zhiqian.zhong@utas.edu.au or ORCID: 0000-0002-1322-5220

[2] Assaad Taoum, School of Engineering, University of Tasmania, Hobart, TAS 7005, Australia, assaad.taoum@utas.edu.au or ORCID: 0000-0002-8294-1909

[3] Nathan Kotlarewski, School of Architecture and Design, University of Tasmania, Launceston, TAS 7250, Australia, nathan.kotlarewski@utas.edu.au or ORCID: 0000-0003-2873-9547

[4] Gregory Nolan, Centre for Sustainable Architecture with Wood, University of Tasmania, Launceston, TAS 7250, Australia, gregory.nolan@utas.edu.au or ORCID: 0000-0002-5846-7012

https://doi.org/10.52202/080513-0145

Eucalyptus nitens (*E. nitens*) is a fast-growing species initially cultivated for the pulp industry but is now gaining attention in the production of various engineered wood products (EWP) [9, 10]. Its rapid growth and potential to meet the increasing demand for sustainable construction timber make it a promising alternative to traditional construction materials [11]. However, integrating *E. nitens* into modern composite systems presents unique challenges, particularly regarding its interaction with fasteners such as screws. A deeper understanding of how screw geometry interacts with the unique properties of *E. nitens* is essential to optimising fastening systems and ensuring structural reliability.

This study investigates the influence of screw geometry, specifically, the effective screw thread bearing area per flank, the thread angle and the screw-grain angle on the axial slip performance. By providing insights into the design and selection of fastening systems, this research contributes to the broader objective of improving the performance and durability of timber-based composite structures, thereby advancing the industry's sustainability goals.

2 – MATERIALS AND METHODS

2.1 TIMBER SPECIMEN PREPARATION

Timber specimens were *E. nitens* sourced from fibre-managed plantation in Tasmania, Australia. The specimens had cross-sectional dimensions of 75 mm × 25 mm, and each sawn board was cut to a length of 220 mm to accommodate two screws and satisfy the minimum requirements specified in AS 1649 [12] and EN 1382 [13]. A total of 175 sawn board specimens were initially sorted according to the fibre grain angle in the cross-section and subsequently grouped according to the screw-grain angle, as outlined in Table 1.

Table 1. Screw-grain angle groups.

Screw-grain angle Group	Screw-grain angle range (θ)
A	$0° \le \theta < 30°$
B	$30° \le \theta < 60°$
C	$60° \le \theta \le 90°$

In addition to the sawn boards, *E. nitens* two- and three-layer glued laminated timber (GLT) were also prepared for the withdrawal testing. To ensure consistency in timber properties across layers, 75 mm × 25 mm timber boards were cut into 220 mm lengths and tagged to maintain traceability within the same board. Then the fibre grain angle for each timber layer was measured and the average fibre grain angle of each GLT specimen was calculated. A total of 60 two-layer GLT specimens and 54 three-layer GLT specimens were sorted and grouped by the screw-grain angle ranges listed in Table 1.

According to the specification of AS 1649 [12] and EN 1382 [13], the minimum screw spacing along the timber grain and end distance was set at 10d, the minimum edge distance at 5d, and the minimum support distance at 3d. All timber specimens were labelled and marked, as illustrated in Fig. 1.

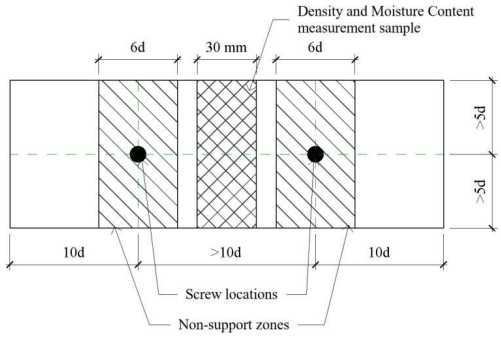

Figure 1. Layout of Specimen Preparation for Density, Moisture Content, and Screw Placement Measurements (Plan View)

Additionally, a 30 mm-wide section was extracted from the middle of each withdrawal test specimen, as shown in Fig. 1, for measuring the timber density (ρ) and moisture content (MC) using over-dried method in accordance with AS/NZS 1080.1 [14] and AS/NZS 1080.3 [15] after the withdrawal testing. The MC, density and density at 12% MC (ρ_{12}) characteristics of the tested specimens are summarised in Table 2. The timber specimen groups E1, E2 and E3 correspond to sawn boards, two-layer GLT and three-layer GLT, respectively.

Table 2 indicates that the three specimen groups exhibited a wide range of timber densities, from 400 kg/m³ to 800 kg/m³. The average density of both E1 and E2 was 600 kg/m3, whereas E3 had a lower average density of 540 kg/m³, approximately 10% lower than E1 and E2.

Table 2. Summary of E. nitens density and moisture content.

Sample Name	Specimen Size	MC (%)				Density (kg/m3)				Density at 12% MC (kg/m3)			
		Avg.	Std.	Min.	Max.	Avg.	Std.	Min.	Max.	Avg.	Std.	Min.	Max.
E1	175 (174)	9.99	0.77	8.36	12.26	600	77	460	810	610	77	470	820
E2	60 (60)	9.68	0.44	8.71	10.50	600	62	470	700	610	63	480	720
E3	54 (54)	9.49	0.94	8.61	15.68	540	73	430	740	560	73	440	750

https://doi.org/10.52202/080513-0145

2.2 SCREW TYPES AND THREAD GEOMETRIC PARAMETERS

In this study, the thread geometric parameters of 15 screws of each type of decking screw and timber screw were measured, and average values were calculated. The thread geometric parameters of SPAX screws are specified in ETA-12/0114 [16].

The study examined two types of decking screws, G8 ($d_o = 4.36\,mm$) and G10 ($d_o = 4.96\,mm$), with effective thread bearing area per flank (A_b) of 11 mm^2 and 14 mm^2, respectively. Additionally, one type of timber screw, G14 ($d_o = 6.46\,mm$, $A_b = 19\,mm^2$), was analysed. Three types of screws from SPAX SP5 ($d_o = 5.1\,mm$), SP6 ($d_o = 6.1\,mm$) and SP8 ($d_o = 8.1\,mm$) with A_b of 12 mm^2, 18 mm^2 and 32 mm^2, respectively, were also tested. The thread angle of decking screws and timber screws was 60°, while the SPAX screws had a thread angle of 35°. The screw thread geometry is shown in Fig. 2.

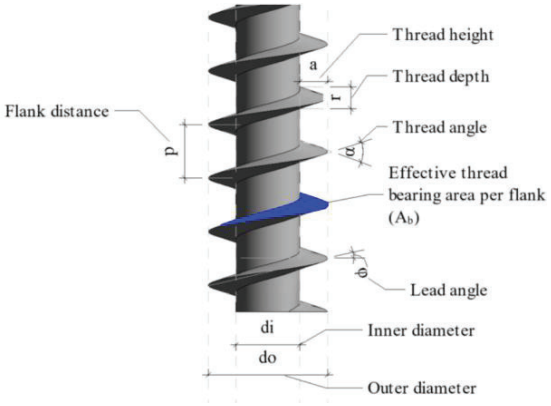

Figure 2. Screw thread geometry

2.3 SCREW PULL-OUT EXPERIMENT

To investigate the effective screw thread bearing area per flank, the thread angle, and the screw-grain angle on the axial slip performance, a minimum of 8 screw specimens in each testing group were loaded along their axis using a Universal Testing Machine (UTM) following EN 1382 [13] instead of following EN 26891 [17] as the latter specifies lateral loading.

A linear variable differential transformer (LVDT) and a linear potentiometer (LP) were attached near the screw head and screw tip, respectively, at the bottom of the timber board, as illustrated in Fig. 3. The LP was installed to account for any initial mechanical gap between the testing frame and specimen.

The axial slip performance of screws in timber was evaluated using the axial slip modulus ($K_{SLS,ax}$), which was determined as the slope of the load-displacement curve recorded during the experiment. The modulus was calculated within the force range of 15% to 40% of the maximum pull-out force ($0.15F_{max}$ to $0.4F_{max}$) using (1) [17-19].

After the pull-out test, a 30 mm of small specimen from each tested specimen was cut to measure its MC and density using the oven-dried method, following AS/NZS 1080.1 [14] and AS/NZS 1080.3 [15].

$$K_{SLS,ax} = \frac{F_{0.4} - F_{0.15}}{\Delta_{0.4} - \Delta_{0.15}} \qquad (1)$$

Where:

- $K_{SLS,ax}$ Axial slip modulus. (kN/mm)
- $F_{0.15}$ 15% of maximum pull-out force. (kN)
- $F_{0.4}$ 40% of maximum pull-out force. (kN)
- $\Delta_{0.15}$ Screw slip in timber at $0.15F_{max}$. (mm)
- $\Delta_{0.4}$ Screw slip in timber at $0.4F_{max}$. (mm)

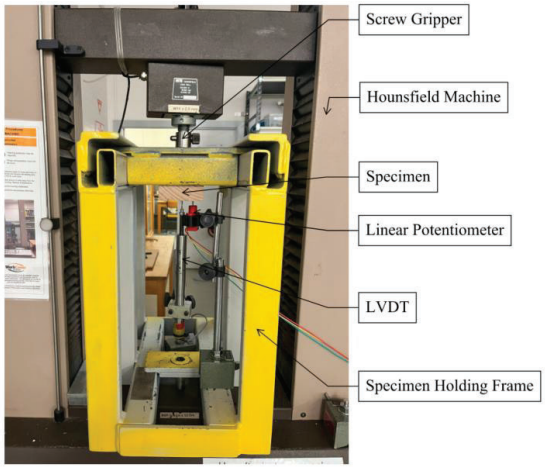

Figure 3. Pull-out experiment setup

3 – RESULTS

Fig. 4 presents the load-displacement curve for the SP5 screw with an effective penetration depth of 25 mm in screw-grain angle Group C timber. This curve characterises the typical pull-out behaviour observed during experimental testing. The axial slip modulus ($K_{SLS,ax}$) is represented by the slope of the initial linear segment of the curve, reflecting the stiffness of the screw-timber connection within the elastic range.

Fig. 5 illustrates the density distribution of the tested GLT layers and categorised by screw thread bearing area. The E1 and E2 timber series exhibit relatively consistent density distributions, with average values around 600 kg/m³ for all tested screw types. However, the E3 timber series displays lower average density values, ranging between 500 kg/m³ and 550 kg/m³.

https://doi.org/10.52202/080513-0145

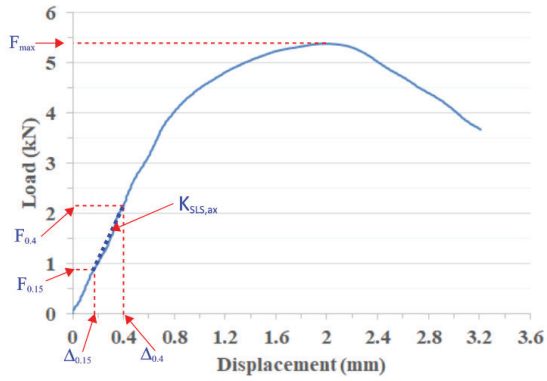

Figure 4. Load-displacement curve of SP5 screw with an effective penetration length of 25 mm in screw-grain angle group C.

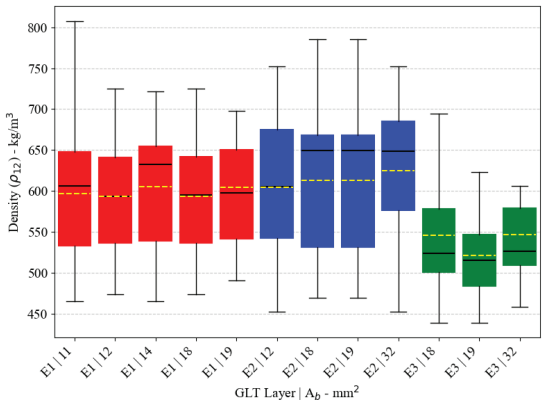

Figure 5. Relation between density at 12% MC and effective thread bearing area per flank in different layers of E. nitens GLT.

Fig. 6 demonstrates that an increase in the effective penetration length of screws in timber enhances axial slip performance, represented by the axial slip modulus ($K_{SLS,ax}$). The E1, E2 and E3 timber series correspond to effective penetration lengths of 25 mm, 50 mm, and 75 mm, respectively. Despite E1 and E2 timber series exhibiting similar timber densities at 12% (Fig. 5), Fig. 6 indicates that E1 timber series has consistently lower average axial slip modulus compared to E2 and E3 timber series. This suggests that shorter penetration lengths result in reduced axial slip performance.

Within E1 timber series, screws with thread bearing areas of 12 mm² and 18 mm² correspond to SPAX SP5 and SP6 screws (SP-series), featuring a 35° thread angle, while the remaining screws belong to the G-series, which have a 60° thread angle. The results indicate that SP-series screws outperform G-series screws in axial slip performance for the same penetration length, suggesting that a smaller thread angle enhances axial slip performance. Furthermore, within the same screw series, a larger thread bearing area correlates with an improved axial slip modulus.

In E2 series, where screws penetrate a two-layer GLT, an increase in effective penetration length leads to a corresponding rise in axial slip modulus. A similar trend is observed within this series, demonstrating that screws with a larger thread bearing area exhibit better axial slip performance.

The E3 series, presenting the longest penetration length, achieves the highest average axial slip modulus among the three groups. Despite the E3 series having the lowest timber density, it still demonstrates the best axial slip performance in three timber series. This confirms that the effective screw penetration length and the screw thread bearing area play a critical role in enhancing axial slip modulus, while timber density also contributes positively to screw axial slip performance. Consistent with previous observations, screws with a larger thread bearing area exhibit higher axial slip modulus values across all timber series.

Overall, the results highlight a positive correlation between timber density, effective penetration length, screw thread bearing area, and axial slip modulus. In contrast, thread angle appears to have a negative impact on axial slip performance, with smaller thread angles resulting in higher axial slip modulus values.

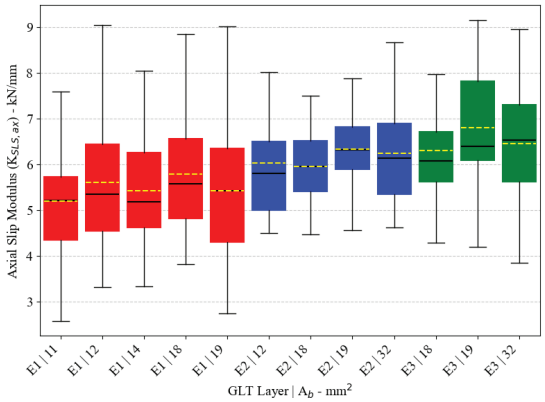

Figure 6. Relation between axial slip modulus and effective thread bearing area per flank in different layers of E. nitens GLT.

Fig. 7 explores the relationship between screw axial slip modulus and screw thread bearing area across different screw-grain angle groups. In E1 timber series, SP-series screws ($A_b = 12\ mm^2$ and $A_b = 18\ mm^2$) generally exhibit better axial slip performance than the G-series screws. Within screw-grain angle Group A, the G-series screw with $A_b = 14\ mm^2$, achieves the highest axial slip modulus, followed by a sharp decrease as the thread bearing area increases.

In screw-grain angle Group B in E1 timber series, the effect of thread bearing area on axial slip modulus remains consistent between the SP-series and G-series screws. As the screw-grain angle increases to Group C,

ranging from 60° to 90°, the axial slip modulus improves with increasing thread bearing area. Additionally, screws with a smaller thread angle provide better axial slip performance.

Notably, only the screw with $A_b = 11\ mm^2$ achieves a peak axial slip modulus in Group B (between 30° and 60°), whereas for other screws, the screw-grain angle generally has a positive effect on axial slip modulus. The relationship between screw-grain angle and axial slip modulus may follow a parabolic trend, where the sensitivity of axial slip modulus to variations in screw-grain angle (i.e., the spread of the parabolic shape) is likely influenced by screw thread bearing area, effective penetration length, and thread angle.

In E2 timber series, screws have an increased effective penetration length. The effect of thread bearing area on axial slip modulus becomes less pronounced. This could be attributed to the combined influence of effective penetration length, thread bearing area, thread angle, and screw-grain angle, which act simultaneously on axial slip modulus.

In E3 timber series, where screws penetrate three GLT layers, the SP-series screws SP6 and SP8 ($A_b = 18\ mm^2$ and $A_b = 32\ mm^2$) feature a 35° thread angle, while the G-series screw ($A_b = 19\ mm^2$) has a 60° thread angle. The results indicate that screws with a larger thread angle and greater effective penetration length are less sensitive to changes in axial slip modulus due to variations in screw-grain angle.

For screws with the same thread angle, the relationship between screw-grain angle and axial slip modulus follows a parabolic trend. Screws with a smaller thread bearing areas (for example, $A_b = 18\ mm^2$ in E3 timber series, 75 mm penetration) exhibit a narrower parabolic shape, meaning their axial slip modulus is more sensitive to screw-grain angle, with rapid changes as the screw-grain angle increases.

Screw with larger thread bearing areas (for example, $A_b = 32\ mm^2$ in E3 timber series, 75 mm penetration) demonstrate a boarder parabolic shape. Although the screw-grain angle negatively affects the axial slip modulus in these screws, the effect occurs in the declining phase of the parabolic trend. the rate of decline is slower compared to screws with a smaller thread bearing area. These findings enhance observations from E1 timber series, further supporting the assumption that the influence of screw-grain angle on axial slip modulus follows a parabolic trend, with its sensitivity governed by thread bearing area, effective penetration length, and thread angle.

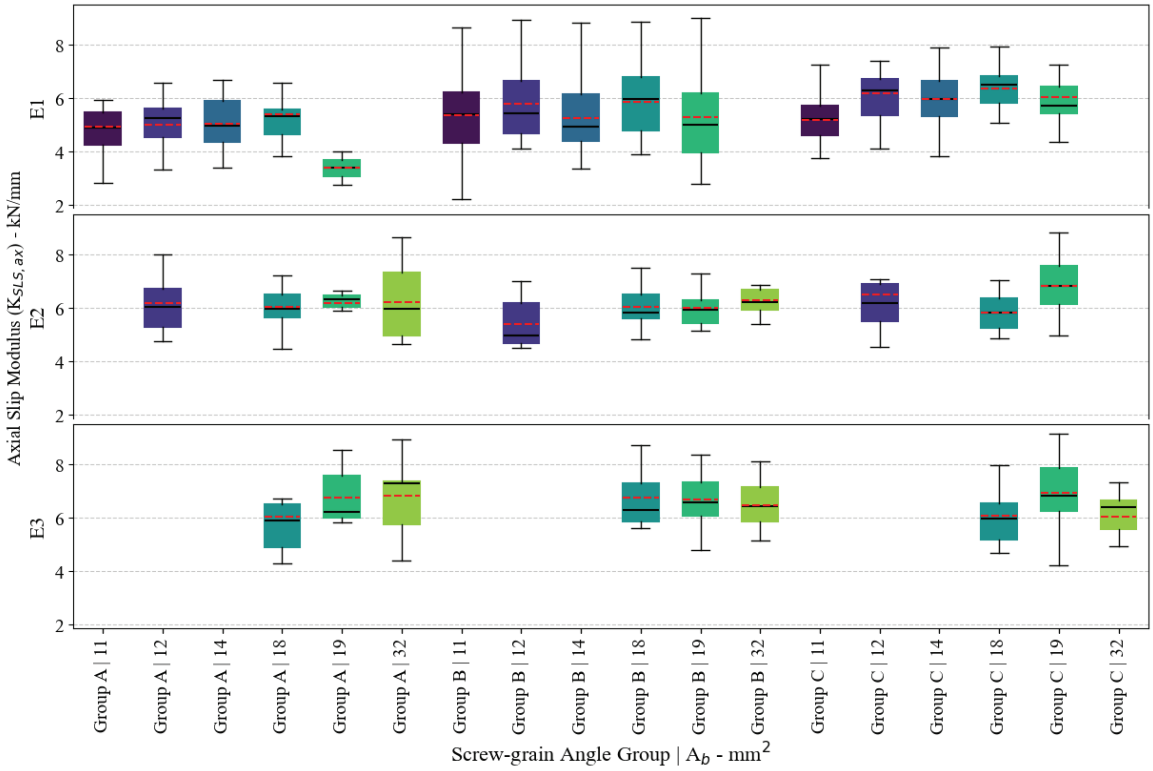

Figure 7. Relation between axial slip modulus and screw-grain angle group for each type of effective thread bearing area per flank in different layers of E. nitens GLT.

https://doi.org/10.52202/080513-0145

4 – CONCLUSIONS

This study investigated the influence of effective screw thread bearing area per flank, thread angle, effective penetration length, screw-grain angle and density on the axial slip performance of screws embedded in *E. nitens*. The study examined six types of screws (G8, G10, SP5, SP6, G14 and SP8), with thread bearing areas ranging from 11 mm^2 to 32 mm^2, effective penetration lengths of 25 mm, 50 mm and 75 mm, with screw-grain angles varying from 0° to 90°. A total of 544 screws in timber were loaded in pull-out using a UTM, including 343 valid screw specimens in *E. nitens* sawn boards, 111 valid screw specimens *E. nitens* two-layer GLT and 90 valid screw specimens *E. nitens* three-layer GLT, in accordance with EN 1382 [13]. The findings highlight key relationships these factors and the axial slip modulus.

The results demonstrate that increasing effective penetration length enhances axial slip performance. Across all tested GLT layers (E1, E2, and E3), screws with greater penetration depths exhibited higher axial slip modulus values. This effect was particularly evident in the E3 series, where screws penetrated three GLT layers (75 mm), resulting in the highest average axial slip modulus. Despite the lower timber density in the E3 timber series compared to E1 and E2, the enhanced axial slip performance suggests that screw penetration length is a more dominant factor than timber density in improving axial slip resistance.

Additionally, the screw thread bearing area significantly influenced axial slip performance. Screws with larger thread bearing areas consistently exhibited higher axial slip modulus values in the same thread angle. This trend was observed across all timber series and was particularly pronounced in the E1 and E2 series, where timber density remained consistent. Among screws of the same type, those with larger thread bearing areas outperformed those with smaller bearing areas, confirming its contribution to axial slip resistance.

Thread angle was found to negatively influence axial slip performance. SPAX screws, featuring a 35° thread angle, generally exhibited higher axial slip modulus compared to G-series screws with a 60° thread angle. This effect was consistent across all penetration lengths, with SPAX screws demonstrating greater axial stiffness in the screw-timber connection under pull-out force. The findings suggest that smaller thread angles enhance axial slip performance by increasing thread loading surface and reducing localised damages in the surrounding timber.

The study also revealed that the relationship between screw-grain angle and axial slip modulus follows a parabolic trend. In screw-grain angle Group A (0° to 30°), axial slip modulus increased with increasing screw-grain angle, reaching a peak in Group B (30° to 60°), before declining in Group C (60° to 90°). This pattern was particularly evident in screws with smaller thread bearing areas and shorter penetration lengths, where axial slip modulus was more sensitive to screw-grain angle variations. In contrast, screws with larger thread bearing areas exhibited a broader parabolic shape, indicating reduced sensitivity to changes in screw-grain angle.

Overall, the study establishes that effective penetration length, thread bearing area, and thread angle are key parameters influencing axial slip performance in *E. nitens*. While timber density contributes positively to screw slip resistance, its effect is secondary to penetration depth and thread geometry. The findings underscore the importance of selecting screws with larger thread bearing areas and smaller thread angles to optimise connection stiffness, particularly in applications where high axial slip resistance is required.

5 – REFERENCES

[1] J. Estévez-Cimadevila, E. Martín-Gutiérrez, F. Suárez-Riestra, D. Otero-Chans, and J. A. Vázquez-Rodríguez, "Timber-concrete composite structural flooring system," (in English), *J. Build. Eng.,* Article vol. 49, 2022, Art no. 104078, doi: 10.1016/j.jobe.2022.104078.

[2] S. C. Auclair, L. Sorelli, and A. Salenikovich, "A new composite connector for timber-concrete composite structures," *Constr Build Mater,* vol. 112, pp. 84-92, 2016/06/01/ 2016, doi: https://doi.org/10.1016/j.conbuildmat.2016.02.025.

[3] *EAD 130118-00-0603. Screws for use in timber constructions.* , European Organisation for Technical Assessment (EOTA), 2016.

[4] B. Shi, W. Liu, H. Yang, and X. Ling, "Long-term performance of timber-concrete composite systems with notch-screw connections," *Eng. Struct.,* vol. 213, p. 110585, 2020/06/15/ 2020, doi: https://doi.org/10.1016/j.engstruct.2020.110585.

[5] C. Zhang and P. Gauvreau, "Timber-Concrete Composite Systems with Ductile Connections," *J Struct Eng,* vol. 141, no. 7, p. 04014179, 2015, doi: doi:10.1061/(ASCE)ST.1943-541X.0001144.

[6] Y. De Santis and M. Fragiacomo, "Timber-to-timber and steel-to-timber screw connections: Derivation of the slip modulus via beam on elastic foundation model," *Eng. Struct.,* vol. 244, p. 112798, 2021/10/01/ 2021, doi: https://doi.org/10.1016/j.engstruct.2021.112798.

[7] *Eurocode 5 : design of timber structure*, British Standards Institution, Brussels, 2004.

[8] R. Tomasi, A. Crosatti, and M. Piazza, "Theoretical and experimental analysis of timber-to-timber joints connected with inclined screws," *Constr Build Mater,* vol. 24, no. 9, pp. 1560-1571, 2010/09/01/ 2010, doi: https://doi.org/10.1016/j.conbuildmat.2010.03.007.

[9] J. Hou, A. Taoum, N. Kotlarewski, and G. Nolan, "Study on the Effect of Finger-Joints on the Strengths of Laminations from Fiber-Managed Eucalyptus nitens," *Forests,* vol. 14, no. 6, p. 1192, 2023. [Online]. Available: https://www.mdpi.com/1999-4907/14/6/1192.

[10] Y. Liang, A. Taoum, N. Kotlarewski, A. Chan, and D. Holloway, "Behavior of Cross-Laminated Timber Panels Made from Fibre-Managed Eucalyptus nitens under Short-Term Serviceability Loads," *Buildings,* Article vol. 13, no. 1, 2023, Art no. 245, doi: 10.3390/buildings13010245.

[11] M. Gutierrez, A. Ettelaei, N. Kotlarewski, and M. Lee, "Structural Properties of Commercial Australian Plantation Hardwood CLT," *Buildings,* Article vol. 13, no. 1, 2023, Art no. 208, doi: 10.3390/buildings13010208.

[12] *AS 1649: Timber: Methods of test for mechanical fasteners and connectors: Basic working loads and characteristic strengths*, Standards Australia International Ltd, 2001.

[13] *BS EN 1382: Timber Structures: Test methods: Withdrawal capacity of timber fasteners*, The British Standards Institution, 2016.

[14] *AS/NZS 1080.1: Timber: Methods of test: Method 1: Moisture content*, Standards Australia International Ltd, 2012.

[15] *AS/NZS 1080.3: Timber: Methods of test : Method 3: Density*, Standards Australia International Ltd, 2000.

[16] *ETA-12/0114: European Technical Approval for SPAX self-tapping screws for use in timber structures. ,* ETS-Denmark A/S, 2020.

[17] *BS EN 26891: Timber Structures: Joints made with mechanical fasteners: General principles for the determination of strength and deformation characteristic.*, The British Standards Institution, 1991.

[18] Y. Zhao, Y. Yuan, Y. Wu, C.-L. Wang, and S. Meng, "Experimental study on the withdrawal performance of mortar-glulam hybrid anchored screws," *Constr Build Mater,* vol. 406, p. 133439, 2023/11/24/ 2023, doi: https://doi.org/10.1016/j.conbuildmat.2023.133439.

[19] *ASTM D5652-15; Standard Test Methods for bolted CONNECTIONS in Wood and Wood-Based Products*, ASTM Committee on Standards, West Conshohocken, United Stastes, 2015.

https://doi.org/10.52202/080513-0145